International Journal of Bifurcation and Chaos, Vol. 30, No. 5 (2020) 2050067 (12 pages)

DOI: 10.1142/S0218127420500674

Time-Reversible Chaotic System with Conditional Symmetry

Chunbiao Li*
Jiangsu Collaborative Innovation Center of Atmospheric Environment and Equipment Technology (CICAEET), Nanjing University of Information Science and Technology, Nanjing 210044, P. R. China
Jiangsu Key Laboratory of Meteorological Observation and Information Processing, Nanjing University of Information Science and Technology, Nanjing 210044, P. R. China
goontry@126.com
chunbiaolee@nuist.edu.cn

Julien Clinton Sprott
Department of Physics, University of Wisconsin–Madison, Madison, WI 53706, USA
sprott@physics.wisc.edu

Yongjian Liu
Guangxi Colleges and Universities Key Laboratory of Complex System Optimization and Big Data Processing, Yulin Normal University, Yulin, Guangxi 537000, P. R. China
liuyongjianmaths@126.com

Received March 7, 2019; Revised September 14, 2019

When the polarity reversal induced by offset boosting is considered, a new regime of a time-reversible chaotic system with conditional symmetry is found, and some new time-reversible systems are revealed based on multiple dimensional offset boosting. Numerical analysis shows that the system attractor and repellor have their own dynamics in respective time domains which constitutes the fundamental property in a time-reversible system. More remarkably, when the conditional symmetry is destroyed by a slightly mismatched offset controller, the system undergoes different bifurcations to chaos, and the corresponding coexisting attractors and repellors shape their own phase trajectories.

Keywords: Time-reversible conditional symmetry; offset boosting; chaotic attractor; chaotic repellor.

*Author for correspondence

1. Introduction

Time-reversible dynamical systems have special dynamics providing an effective approach for the observation of coexisting attractors and repellors. As reported in [Sprott, 2015], time-reversible symmetric chaotic ODE systems have symmetric chaotic repellors when the time is reversed. Generally, for those chaotic systems with a quadratic nonlinearity, the existence of a trajectory in forward time does not imply its existence in backward time [Leonov & Kuznetsov, 2015]. However, for those symmetric systems with a symmetric pair of coexisting attractors, a plane of equilibria can be introduced to convert one of the coexisting attractors to a repellor in positive time [Li *et al.*, 2017], and consequently, those systems become time-reversible ones. A chaotic system with conditional symmetry can be constructed from a unique structure, where the symmetry is recovered by single or multiple dimensional offset boosting [Li *et al.*, 2017; Li *et al.*, 2018]. The fundamental reason is that offset boosting of a variable can provide polarity reversal for some functions of that variable on the right-hand side of the equation without revising the variable polarity on the left-hand side. Following this idea, for a time-reversible symmetric system, the polarity imbalance induced by the time reversal can be restored if some of the variables have their polarity reversed from offset boosting. Figure 1 shows the structural property based on polarity balance according to the symmetry in chaotic systems [Lai *et al.*, 2017; Lai & Chen, 2016a, 2016b; Bao *et al.*, 2016; Chen *et al.*, 2017; Hoover *et al.*, 1996; Sprott, 2014; Zhou *et al.*, 2016; Wang *et al.*, 2017; Zhou *et al.*, 2017; Zhou *et al.*, 2018a; Zhou *et al.*, 2018b; Jafari *et al.*, 2015; Wei *et al.*, 2014; Liu & Pang, 2011]. Attractors and repellors in time-reversible systems are in separate time domains (forward time or backward time) and have some connections with one another. It is still undetermined whether a dynamical system has both a convergent attractor and repellor since in most cases one of them is divergent.

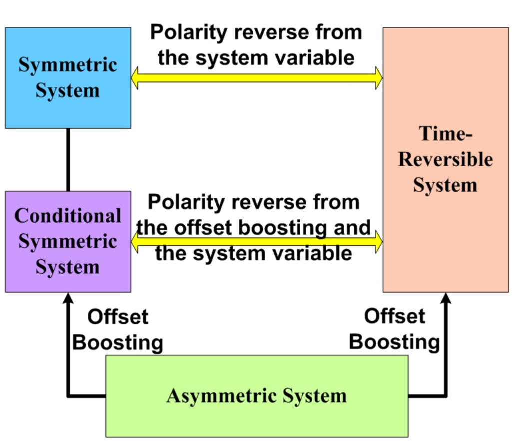

Fig. 1. Polarity reversal for system structure reconstruction.

In this work, comprehensive polarity reversal is considered, which is from offset boosting along with time and variable reversal, and therefore a new series of time-reversible chaotic systems with conditional symmetry is constructed. All the newly found time-reversible systems provide coexisting convergent attractors and repellors. The general law hidden in coexisting attractors and repellors is revealed by further bifurcation analysis. In the paper, we give some new structures of time-reversible chaotic systems in Sec. 2 where one-dimensional or two-dimensional offset boosting is introduced for polarity balance. Some new chaotic systems in this regime are proposed in Sec. 3. Bifurcation analysis in positive time and negative time is given for finding asymmetric attractors and repellors in Sec. 4. In the last section, a general discussion and conclusion is made about the dynamics hidden in time-reversible chaotic systems.

2. Offset Boosting for Time Reversible Conditional Symmetry

Definition 2.1. For a dynamical system $\dot{X} = F(X) = (f_1(X), f_2(X), \ldots, f_N(X))$ $(X = (x_1, x_2, \ldots, x_N))$, if there exists a variable substitution including polarity reversal and offset boosting such as $u_{i_1} = -x_{i_1}, u_{i_2} = -x_{i_2}, \ldots, u_{i_k} = -x_{i_k}$, $u_{j_1} = x_{j_1} + d_{j_1}, u_{j_2} = x_{j_2} + d_{j_2}, \ldots, u_{j_l} = x_{j_l} + d_{j_l}$, $u_m = x_m$, $t \to -t$ (here $1 \leq i_1, \ldots, i_k \leq N$, $1 \leq j_1, \ldots, j_l \leq N$, $i_1, \ldots, i_k$ and $j_1, \ldots, j_l$ are not identical, $m \in 1, 2, \ldots, N \backslash i_1, \ldots, i_k, j_1, \ldots, j_l$), the derived system will retain its balance of polarity on the two sides of the equation and will satisfy $\dot{U} = F(U)$ $(U = (u_1, u_2, \ldots, u_N)$, then the system $\dot{X} = F(X)$ $(X = (x_1, x_2, \ldots, x_N)))$ is defined as one of l-dimensionally *time-reversible conditional symmetry* since the polarity balance is from l-dimensional offset boosting [Li & Sprott, 2016a; Li *et al.*, 2016; Li *et al.*, 2018; Bao *et al.*, 2018].

Although chaotic systems with time-reversible conditional symmetry can be obtained from those with conditional symmetry by introducing a new plane of equilibria, the tending-to-overstaffed structure makes the dynamic observation more turbid. In the following, new elegant cases of chaotic systems with time-reversible conditional symmetry are constructed. For example, to obtain a time-reversible conditional reflection symmetric system, suppose there is a polarity reversal for the time t and the system variable x_i. Then the polarity of the variable x_i remains the same, while all the other dimensions need to have polarity balance since the negative time $-t$ introduces a minus sign on the left-hand side, and the terms including the system variable x_i may add new minus signs in some of the terms on the right-hand side, which in turn may require additional minus signs from offset boosting to balance it. That is to say, to keep the polarity balance in the variable x_j, the polynomial equation $f_j(X)$ needs to extract a new minus sign which resorts to new functions from offset boosting without revising the basic dynamics as $f_j(x_1, x_2, -x_i, \ldots, F_{j_1}(x_{j_1}), F_{j_2}(x_{j_2}), \ldots, F_{j_l}(x_{j_l}), \ldots, x_N)$ ($1 \le j_1, \ldots, j_l \le N, j_1, \ldots, j_l$ are not identical, and l is even). Here the polarity reversal from offset boosting $F_{j_m}(x_{j_m} + d_{j_m}) = -F_{j_m}(x_{j_m})$ ($j_1 \le j_m \le j_l$) is a new power to add a minus sign on the right-hand side of the equation without producing any minus sign on the left-hand side since $d(x_{j_m} + d_{j_m}) = d(x_{j_m})$. In the following, we show some examples to see how the polarity imbalance is restored by a suitable offset boosting.

Theorem 2.1. *The following system can be transformed into a new version with time-reversible conditional reflection symmetry with respect to the variable x by introducing a nonmonotonic function $F(y)$ [Li et al., 2017; Li et al., 2019].*

$$\begin{cases} \dot{x} = a_1x^2 + a_2y^2 + a_3xy + a_4z^2 + a_5z + a_6, \\ \dot{y} = a_7x + a_8xz + a_9y + a_{10}yz, \\ \dot{z} = a_{11}x + a_{12}xz + a_{13}y + a_{14}yz. \end{cases} \tag{1}$$

Proof [Proof of Theorem 2.1]. If $x \to -x$, $t \to -t$, the polarity balance of the second and last dimensions of Eq. (1) are destroyed because of the polarity invariance in the variables y and z, while the polarity balance can be restored by a polarity reversal of the variable x and offset boosting in the variable y. Suppose $y \to F(v)$ (here $F(v)$ is nonmonotonic) if $v \to v + c$ leads to $F(v + c) \to -F(v)$, the variable substitution $x \to -x$, $y \to v + c$, $z \to z$, $t \to -t$ will restore the polarity balance in the following equation,

$$\begin{cases} \dot{x} = a_1x^2 + a_2(F(y))^2 + a_3x(F(y)) \\ \qquad + a_4z^2 + a_5z + a_6, \\ \dot{y} = a_7x + a_8xz + a_9(F(y)) + a_{10}(F(y))z, \\ \dot{z} = a_{11}x + a_{12}xz + a_{13}(F(y)) + a_{14}(F(y))z, \end{cases} \tag{2}$$

which proves that system (1) can be transformed into system (2) with time-reversible conditional reflection symmetry by a suitable nonmonotonic function $F(y)$. For the same reason, the following jerk equation,

$$\begin{cases} \dot{x} = y, \\ \dot{y} = z, \\ \dot{z} = a_1x + a_2xy + a_3z + a_4yz, \end{cases} \tag{3}$$

can also be transformed into a new version with time-reversible conditional reflection symmetry since the polarity imbalance from the transformation $x \to -x$, $y \to y$, $z \to z + c$, $t \to -t$ can be recovered by the offset boosting when a suitable nonmonotonic operation $F(z)$ is done with the terms containing the variable z. Meanwhile, the system

$$\begin{cases} \dot{x} = a_1x^2 + a_2y^2 + a_3z^2 + a_4xy \\ \qquad + a_5xz + a_6yz + a_7, \\ \dot{y} = a_8x + a_9y + a_{10}z, \\ \dot{z} = a_{11}x^2 + a_{12}y^2 + a_{13}z^2 + a_{14}xy \\ \qquad + a_{15}xz + a_{16}yz + a_{17}, \end{cases} \tag{4}$$

can be transformed into a system with time-reversible conditional rotational symmetry since the polarity imbalance from the transformation $x \to -x$, $y \to y + c$, $z \to -z$, $t \to -t$ can be recovered by offset boosting of the variable y from a special nonmonotonic operation $F(y)$. ■

We can also transform chaotic flows with the structure of Eqs. (5) and (6) to have time-reversible conditional symmetry if suitable functions like absolute value functions or trigonometric functions

[Li *et al.*, 2017; Li *et al.*, 2019] are introduced in two dimensions for polarity reversal by the offset boosting.

$$\begin{cases} \dot{x} = a_1x^2 + a_2y^2 + a_3z^2 + a_4xy \\ \qquad + a_5xz + a_6yz + a_7, \\ \dot{y} = a_8x + a_9y + a_{10}z, \\ \dot{z} = a_{11}x + a_{12}y + a_{13}z, \end{cases} \tag{5}$$

$$\begin{cases} \dot{x} = y, \\ \dot{y} = z, \\ \dot{z} = a_1x^2 + a_2y^2 + a_3z^2 + a_4xy \\ \qquad + a_5xz + a_6yz + a_7. \end{cases} \tag{6}$$

To recover the balance of polarity governed by the reverse time and one of the variables, 2D offset boosting is necessary to return a minus sign. Suppose $x \to -x$, $y \to y + c_1$, $z \to z + c_2$, $t \to -t$, if $v = y + c_1$ leads to $F(v) = F(y + c_1) = -F(y)$, and $w = z + c_2$ leads to $G(w) = G(z + c_2) = -G(z)$, all the polarity balance can be restored in the revised system, and thus system (5) has 2D time-reversible conditional reflection symmetry. System (6) is a simpler jerk structure where the offset boosting should be introduced in the variables x and y for retaining the polarity balance, and the polarity reversal happens in the variable z to obtain the time-reversible version. Notice that system (6) provides the same structure for constructing either the time-reversible system with conditional reflection symmetry based on 2D offset boosting or the conditional rotational symmetry based on 1D offset boosting [Li *et al.*, 2017; Li *et al.*, 2019]. To expand the list, we here give another case demonstrated by the following.

Remark 2.1. A 3D inversion symmetric system can be transformed into a time-reversible system with conditional symmetry if introducing nonmonotonic functions causes 3D polarity reversal from offset boosting. Specifically, the structure of Eq. (7) is a case such that the nonlinearity $f(x, y, z)$ is an odd function.

$$\begin{cases} \dot{x} = y, \\ \dot{y} = z, \\ \dot{z} = a_1x + a_2y + a_3z + a_4f(x, y, z). \end{cases} \tag{7}$$

The 3D offset boosting returns the polarity balance when each variable on the right-hand side is replaced by a suitable nonmonotone function and time is reversed.

3. New Cases of Time-Reversible Conditional Symmetry

Considering the above six cases, Eqs. (1) and (3) can be transformed into their time-reversible versions producing a symmetric pair of strange attractor and repellor with conditional reflection symmetry by 1D offset boosting, while Eq. (4) can be transformed into a time-reversible system with a conditional rotational symmetric pair of attractor and repellor from a similar 1D offset boosting. Equations (5) and (6) are the source systems for time-reversible conditional reflection symmetry when 2D offset boosting is introduced for restoring polarity balance. Accordingly, Eq. (7) can reach its time-reversible version of conditional inversion symmetry when 3D offset boosting is introduced. All the original chaotic systems (OCSs) are normally asymmetric ones as listed in Table 1, and the corresponding time-reversible conditional symmetric systems (TCSSs) show coexisting symmetric pairs of attractors and repellors.

For obtaining representative Lyapunov exponents rather than absolute ones [Kuznetsov *et al.*, 2018a, 2018b], all the finite-time LEs are computed for the time interval $[0, 10^7]$ for the initial points on the attractor as listed in Table 1. In those systems with nonsmooth right-hand side, for calculating Lyapunov exponents, all the derivatives of the absolute value function are given with signum functions in the Jacobian matrixes [Leonov *et al.*, 2015]. Generally speaking, the ergodicity will help to identify the chaotic attractor [Kuznetsov *et al.*, 2018a, 2018b]. The maximum of the corresponding local Kaplan–Yorke dimensions from a grid of points on the attractor can be helpful for this demonstration. In Table 1, the Kaplan–Yorke dimension is derived from the Lyapunov exponents from the given initial conditions.

Strange attractors in the original asymmetric systems are shown in Fig. 2, five of which are asymmetric. Symmetric pairs of coexisting attractors and repellors in the time-reversible versions of conditional symmetry are shown in Figs. 3–8. Figure 3 shows the coexisting attractor and repellor in TCSS1 induced by 1D offset boosting of the y variable, while Fig. 4 shows such a coexisting pair by offset boosting of the z variable in TCSS2. A conditional rotational symmetric pair of attractor and

Table 1. Original chaotic systems (OCSs) and their corresponding time-reversible versions with conditional symmetry (TCSSs).

Systems	Equations	Parameters	Equilibria	Eigenvalues	LEs	D_{KY}	(x_0, y_0, z_0)
OCS1	$\dot{x} = az^2 + 1$	$a = -0.6$	$(0, 0, 1.2909)$	$-2.3650, 0.6825, \pm 1.1015i$	0.1930	2.1632	$-1, 1, -1$
	$\dot{y} = bxz - y$	$b = 2.76$	$(0, 0, -1.2909)$	$-1.9969, 0.4985, \pm 1.8143i$	0		
	$\dot{z} = -x + y$				-1.1950		
TCSS1	$\dot{x} = az^2 + 1$	$a = -0.6$	$(0, 28, 1.2910)$	$-2.3650, 0.6825, \pm 1.1015i$	0.1100	2.1649	$-4, 1, 0$
	$\dot{y} = bxz - F(y)$	$b = 2.76$	$(0, 28, -1.2910)$	$-1.9970, 0.4950, \pm 1.8142$	0		
	$\dot{z} = -x + y + F(y)$				-0.6663		
	$F(y) = \lvert y \rvert - 28$						
OCS2	$\dot{x} = y$	$a = 0.1$	$(0, 0, 0)$	$-1.0850, 0.0425, \pm 0.3006i$	0.0170	2.0166	$-1.5, 1.5, -2.5$
	$\dot{y} = z$	$b = 0.54$			0		
	$\dot{z} = -ax - bxy - z - yz$				-1.0170		
TCSS2	$\dot{x} = y$	$a = 0.1$	$(0, 0, 0.8)$	$-1.0850, 0.0425, \pm 10.3006i$	0.0170	2.0167	$-1.28, 0.36, 1.04$
	$\dot{y} = F(z)$	$b = 0.54$	$(0, 0, -0.8)$	$1.0850, -0.0425, \pm 0.3006$	0		
	$\dot{z} = -ax - bxy - F(z) - yF(z)$				-1.0170		
	$F(z) = \lvert z \rvert - 0.8$						
OCS3	$\dot{x} = yz$	$a = 18$	$(0, 1, 0)$	$-0.8828, 0.4414, \pm 6.3706i$	0.1450	2.0296	$10, -5, -8$
	$\dot{y} = ax + bz$	$b = 20$	$(0, -1, 0)$	$-6.7340, 0.9194, 5.8145$	0		
	$\dot{z} = -y^2 + z^2 + 1$				-4.9046		
TCSS3	$\dot{x} = F(y)z$	$a = 18$	$(0, 23, 0)$	$-6.7339, 0.9194, 5.8145$	0.1452	2.0296	$10, 25, -6$
	$\dot{y} = ax + bz$	$b = 20$	$(0, 25, 0)$	$-0.8828, 0.4414, \pm 6.3706i$	0		
	$\dot{z} = -(F(y))^2 + z^2 + 1$				4.9056		
	$F(y) = \lvert y \rvert - 24$						

Table 1. (*Continued*)

Systems	Equations	Parameters	Equilibria	Eigenvalues	LEs	D_{KY}	(x_0, y_0, z_0)
OCS4	$\dot{x} = -az^2 + xy$	$a = 3$	$(0, 0, 0)$	$0, 0, \pm 1.0000i$	0.1030	2.0780	$-2, -3, 0$
	$\dot{y} = z$				0		
	$\dot{z} = x - y$				-1.3202		
TCSS4	$\dot{x} = -a(G(z))^2 + xF(y)$	$a = 3$	$(0, 5, 3)$	$0, 0, \pm i$	0.1028	2.0779	$-2, 3, -3$
	$\dot{y} = G(z)$		$(0, -5, 3)$	$-1, 0, 1$	0		
	$\dot{z} = x - F(y)$		$(0, 5, -3)$	$-1, 0, 1$	-1.3199		
	$F(y) = \|y\| - 5$		$(0, -5, -3)$	$0, 0, \pm i$			
	$G(z) = \|z\| - 3$						
OCS5	$\dot{x} = y$	$a = 0.75$	$(-3.1623, 0, 0)$	$-3.5407, 0.1892, \pm 1.1419i$	0.0376	2.0102	$-4, 2, 0$
	$\dot{y} = z$	$b = 3.5$	$(3.1623, 0, 0)$	$3.5407, -0.1892, \pm 1.1419i$	0		
	$\dot{z} = ax^2 - by^2 + xz$	$c = 7.5$			-3.1950		
	$+ yz - c$						
TCSS5	$\dot{x} = G(y)$	$a = 0.75$	$(\pm 10 \pm \sqrt{10}, \pm 4, 0)$	$3.5407, -0.1892, \pm 1.1419i$	0.0367	2.0099	$2, 1, 1$
	$\dot{y} = z$	$b = 3.5$	$(\mp 10 \mp \sqrt{10}, \pm 4, 0)$	$-1.0599, 2.1111, \pm 0.1359i$	0		
	$\dot{z} = a(F(x))^2 - b(G(y))^2$	$c = 7.5$	$(\pm 10 \mp \sqrt{10}, \pm 4, 0)$	$-3.5407, 0.1892, \pm 1.1419i$	-3.6974		
	$+ F(x)z + G(y)z - c$		$(\mp 10 \pm \sqrt{10}, \pm 4, 0)$	$1.0599, -2.1111, \pm 0.1359i$			
	$F(x) = \|x\| - 10$						
	$G(y) = \|y\| - 4$						
OCS6	$\dot{x} = y$	$a = 2.03$	$(0, 0, 0)$	$-2.2310, 0.1005, \pm 0.6619i$	0.0769	2.0365	$0, 0.96, 0$
(*Malasoma System*)	$\dot{y} = z$				0		
	$\dot{z} = -az - x + xy^2$				-2.1069		
TCSS6	$\dot{x} = G(y)$	$a = 2.03$	$(-6, -1.6, -2)$	$2.2309, -0.1005, \pm 0.6619i$	0.0770	2.0365	$0, 0.96, 0$
	$\dot{y} = H(z)$		$(6, -1.6, -2)$	$-0.6149, 1.6725, 0.9724$	0		
	$\dot{z} = -aH(z) - F(x) + F(x)(G(y))^2$		$(-6, 1.6, -2)$	$-0.6149, 1.6725, 0.9724$	-2.1070		
	$F(x) = \|x\| - 6$		$(6, 1.6, -2)$	$2.2309, -0.1005, \pm 0.6619i$			
	$G(y) = \|y\| - 1.6$		$(-6, -1.6, 2)$	$-2.2309, 0.1005, \pm 0.6619i$			
	$H(z) = \|z\| - 2$		$(6, -1.6, 2)$	$0.6149, -1.6725, -0.9724$			
			$(-6, 1.6, 2)$	$0.6149, -1.6725, -0.9724$			
			$(6, 1.6, 2)$	$-2.2309, 0.1005, \pm 0.6619i$			

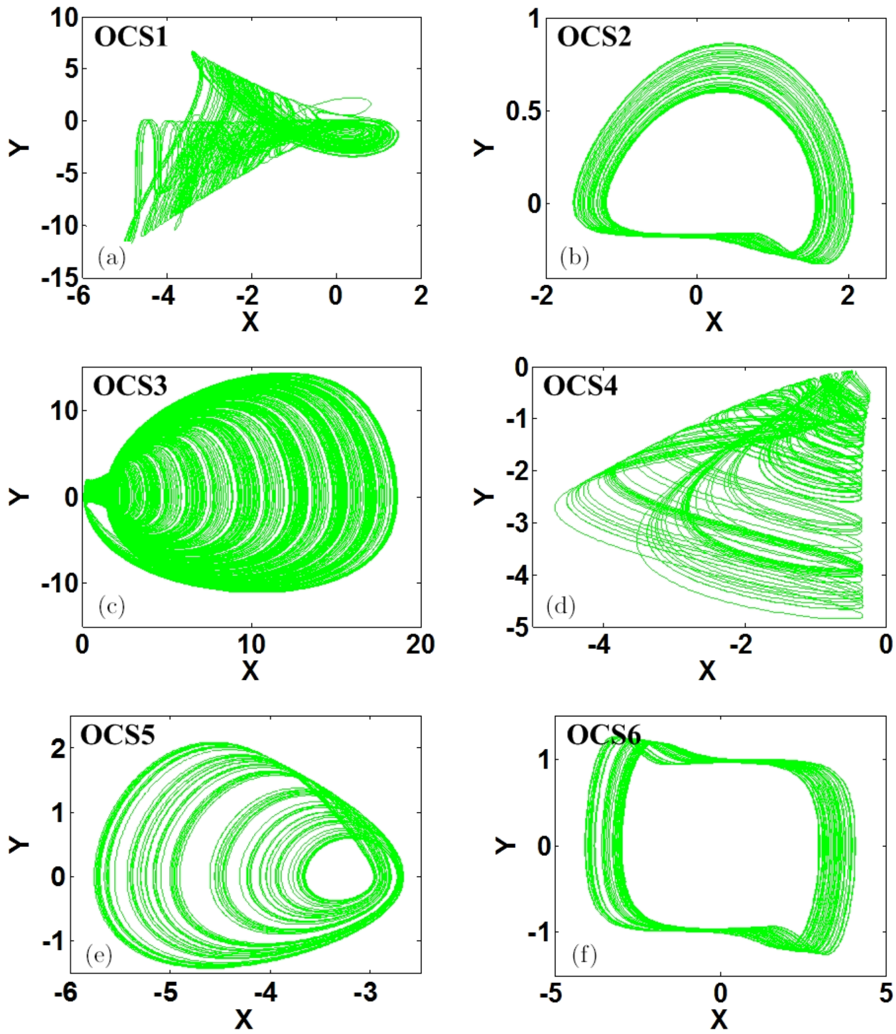

Fig. 2. Strange attractors for the original asymmetric chaotic systems.

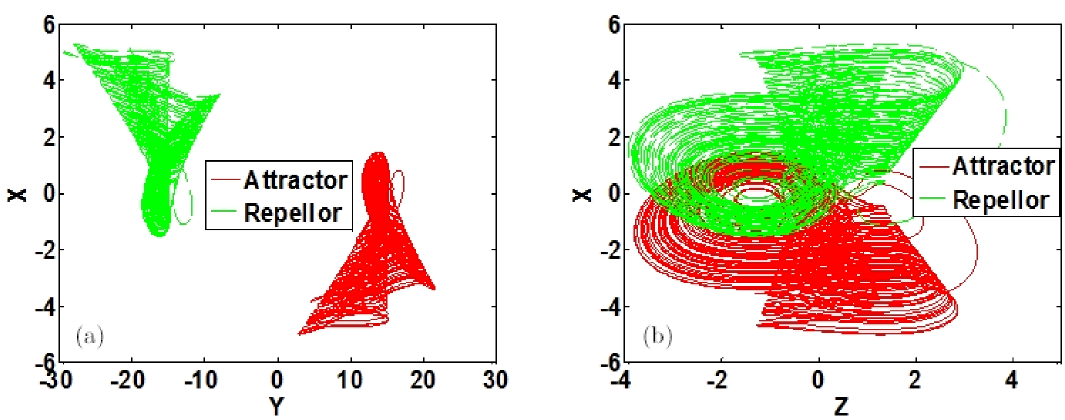

Fig. 3. Strange attractor and repellor with conditional reflection symmetry in system TCSS1 from 1D offset boosting: initial condition $(-4, 1, 0)$ for the attractor and $(-4, -4, 0)$ for the repellor.

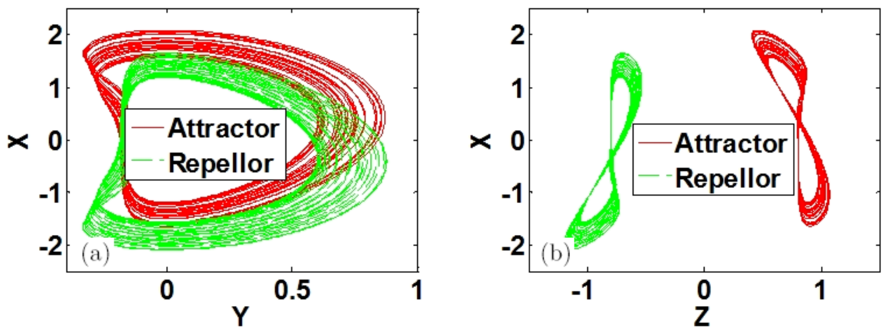

Fig. 4. Strange attractor and repellor with conditional reflection symmetry from 1D offset boosting in system TCSS2: initial condition (−1.28, 0.36, 1.04) for the attractor and (1.28, 0.36, −1.04) for the repellor.

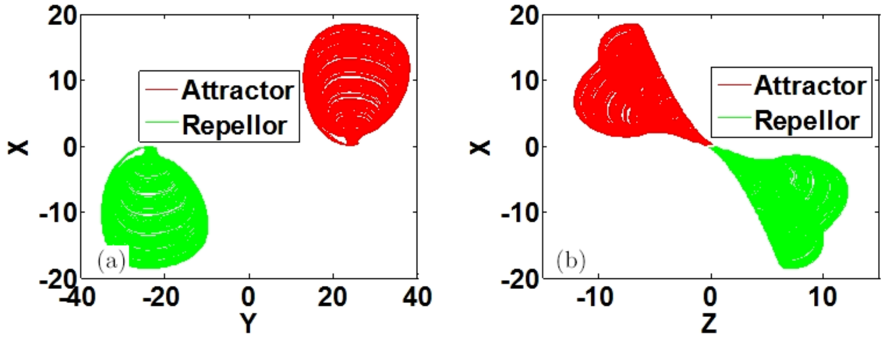

Fig. 5. Strange attractor and repellor with conditional rotational symmetry from 1D offset boosting in system TCSS3: initial condition (10, 25, −6) for the attractor and (−10, −20, 6) for the repellor.

repellor in system TCSS3 is shown in Fig. 5 requiring offset boosting in the y variable. A symmetric pair of attractor and repellor in system TCSS4 from 2D offset boosting of the y and z variables, is shown in Fig. 6. Offset boosting of the variables x and y restores the polarity balance when time is reversed, and system TCSS5 also has a symmetric pair of attractor and repellor as shown in Fig. 7.

More interestingly, inversion symmetric systems also provide an original source for hosting time-reversible versions, where the variable polarity reversal in three dimensions is replaced by the function-based polarity reversal from offset boosting in the negative time domain. As shown in Fig. 8, two sets of chaotic attractors and repellors are captured by selecting different initial conditions.

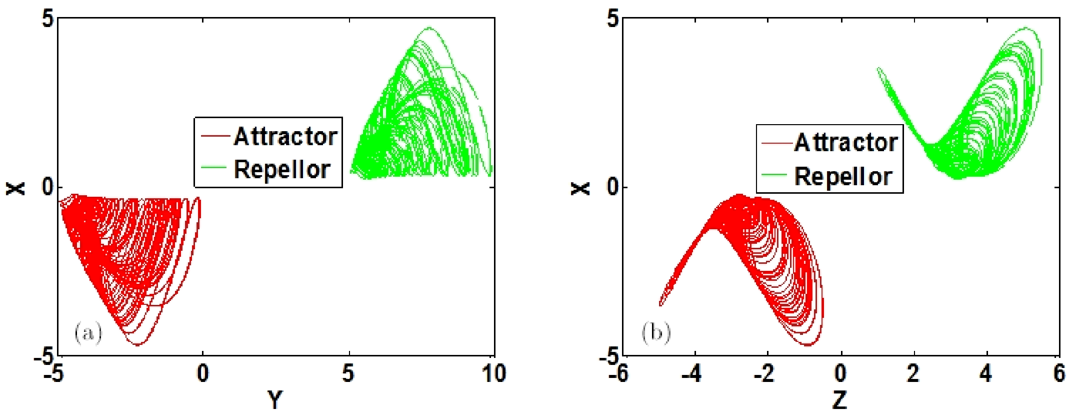

Fig. 6. Strange attractor and repellor with conditional reflection symmetry from 2D offset boosting in system TCSS4: initial condition (−2, 3, −3) for the attractor and (−2, 8, 7) for the repellor.

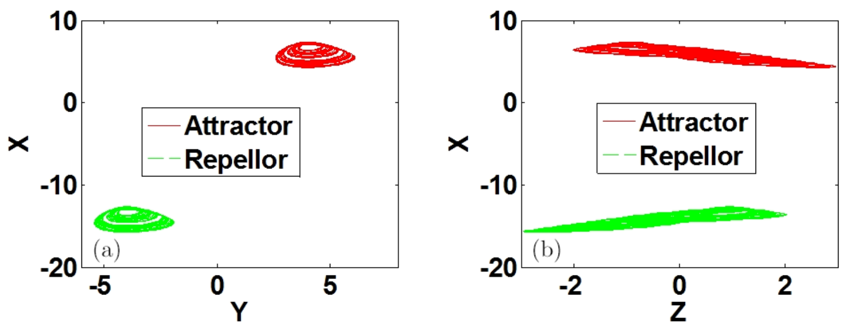

Fig. 7. Strange attractor and repellor with conditional reflection symmetry from 2D offset boosting in system TCSS5: initial condition (2, 1, 1) for the attractor, (−14, −5, −5) for the repellor.

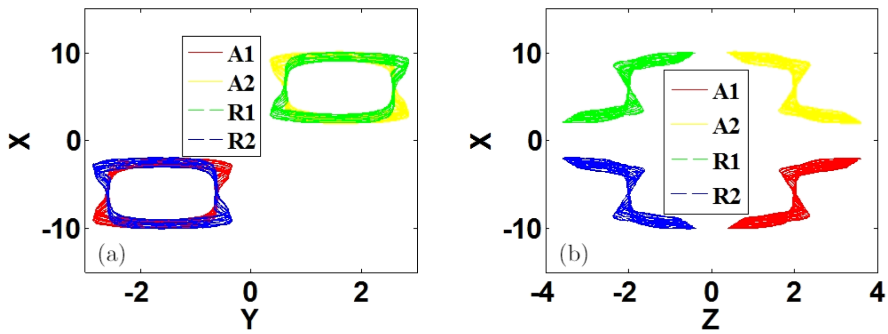

Fig. 8. Strange attractors and repellors with conditional symmetry from 3D offset boosting in system TCSS6: attractors (0, 0.96, 0) for red, (6, 2.56, 2) for yellow, and repellors (0, −0.96, 0) for green, (−6, −2.56, −2) for blue.

As predicted, the coexisting attractors and repellors reside in their separate phase spaces with different offset gaps in one or two dimensions. The reason why two symmetric pairs of attractors and repellors coexist is due to the coexistence of symmetry in the positive time domain and conditional symmetry in the negative time domain. Here the degree of freedom for polarity transformation is three, which includes time polarity, variable polarity, and function polarity. Time polarity revises the sign on the left side of the differential equation; variable polarity changes the polarity balance on both sides of the equation, while the function polarity only modifies the polarity of the right-hand side. Also note that the function polarity reversal may arise from various nonmonotonic functions, which govern the function polarity with different spans of offset boosting. Therefore, new polarity balance may be obtained from different combinations of polarity reversal.

4. Asymmetric Bifurcations in the Domain of Attractor and Repellor

In time-reversible symmetric systems, the attractor is always paired with a corresponding repellor. However, in time-reversible systems with conditional symmetry, those coexisting attractors and repellors appear more freely, especially when the offset constants are different. For example, consider the system TCSS3 with the function $F(y)$ introduced in two terms of the equation. Rewrite the equation as

$$\begin{cases} \dot{x} = F_1(y)z, \\ \dot{y} = ax + bz, \\ \dot{z} = -(F_2(y))^2 + z^2 + 1, \end{cases} \tag{8}$$

where $F_1(y) = |y| - d_1$, $F_2(y) = |y| - d_2$. Normally, the two functions are equal, $F_1(y) = F_2(y)$, which replaces the system variable y for constructing the same dynamics and provides the fundamental condition for conditional symmetry. Bifurcations of the attractor and repellor are almost symmetric in their route to chaos as shown in Fig. 9.

However, when $F_1(y) \neq F_2(y)$, the bifurcations in positive time and negative time are different, producing asymmetric attractors and repellors. As shown in Fig. 10, even a slight deviation in the offset drives system TCSS3 to dramatically different bifurcations. This shows that when $d_1 = 23.6$, $d_2 = 24$, and a varies in $[13.2, 21.2]$, a chaotic attractor

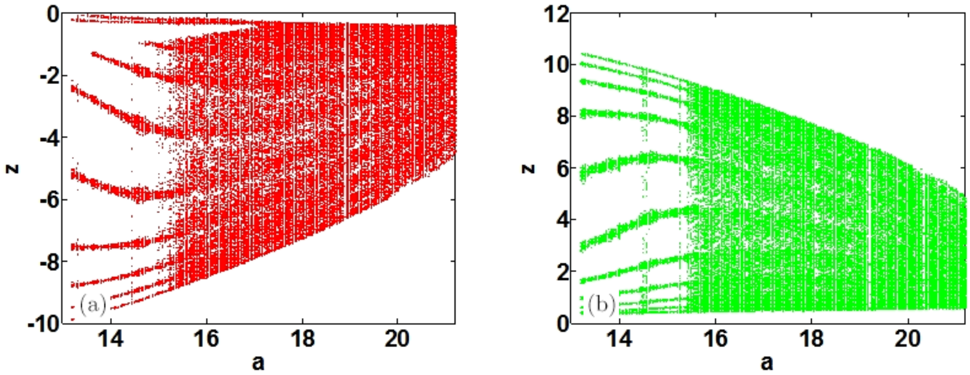

Fig. 9. Symmetric bifurcation in system TCSS3 with $b = 20$, $d_1 = d_2 = 24$ when a varies in $[13.2, 21.2]$: (a) attractor bifurcation with initial condition $(10, 20, -6)$ on the plane of $y = 23.5$ and (b) repellor bifurcation with initial condition $(-10, -20, 6)$ on the plane of $y = -23.5$.

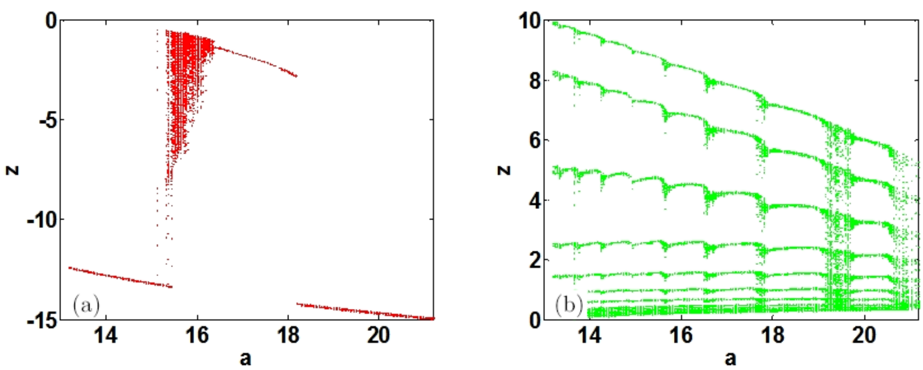

Fig. 10. Asymmetric bifurcation in system TCSS3 with $b = 20$, $d_1 = 23.6$, $d_2 = 24$ when a varies in $[13.2, 21.2]$: (a) attractor bifurcation with initial condition $(10, 20, -6)$ on the plane of $y = 23.5$ and (b) repellor bifurcation with initial condition $(-10, -20, 6)$ on the plane of $y = -23.5$.

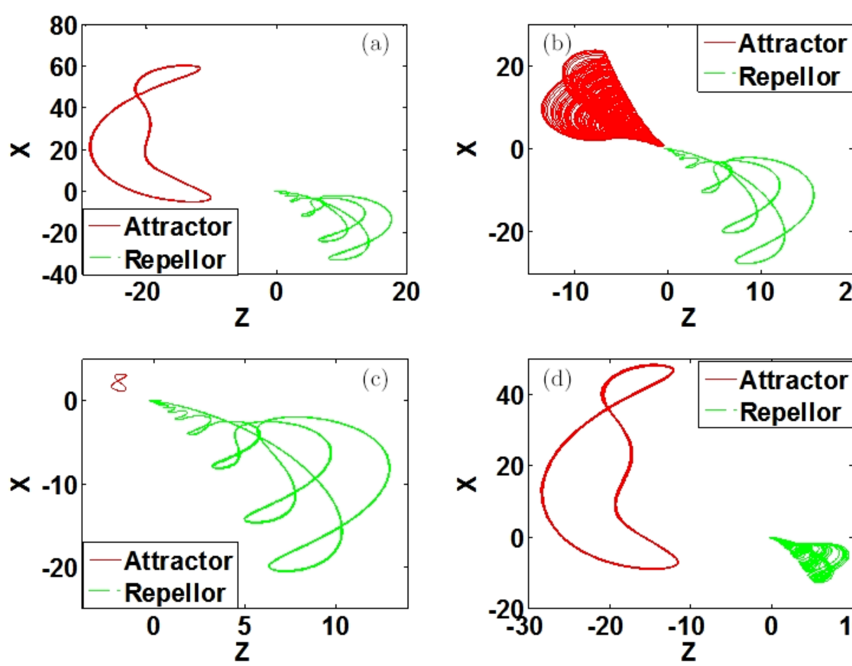

Fig. 11. Coexisting attractors and repellors in system TCSS3 with $d_1 = 23.6$, $d_2 = 24$, the initial condition $(10, 20, -6)$ is for the attractors and the initial condition $(-10, -20, 6)$ is for the repellors: (a) $a = 14.5$, (b) $a = 15.5$, (c) $a = 17$ and (d) $a = 19.5$.

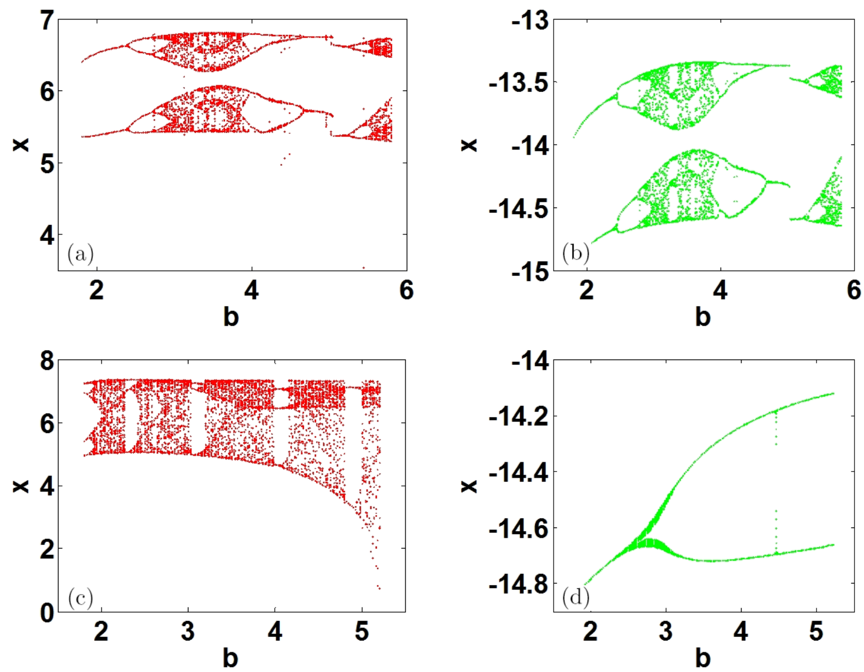

Fig. 12. Bifurcations in system TCSS5 on the plane of $z = 0$ when b varies in $[1.8, 5.3]$: for (a) and (b) $aF_1(x)F_2(x)+F_3(x)z = a(|x| - 10)(|x| - 10) + (|x| - 10)z$ while for (c) and (d) $F_1(x)F_2(x) + F_3(x)z = a(|x| - 10)(|x| - 11) + (|x| - 10)z$; attractor bifurcation is from the initial condition $(2, 1, 1)$ while repellor bifurcation is from the initial condition $(-14, -5, -5)$.

forms in a concentrated area, while a chaotic repellor and a periodic repellor stagger out repeatedly. As shown in Fig. 11, different combinations of coexisting attractors and repellors are observed in their phase spaces. This shows that the repellor is relatively stubborn on changing its structure.

A similar phenomenon occurs in other time-reversible versions. The time-reversible property of system TCSS5 is based on two-dimensional offset boosting. The offset control functions provide more chances for separate bifurcations in the positive and negative time domains. The nonmonotonic function of x exists in the third dimension, and can be rewritten as $aF_1(x)F_2(x) + F_3(x)z$. Slightly unbalanced offset constants drive TCSS5 to different dynamics in positive and negative time. Figures 12(a) and 12(b) indicate that coexisting attractors and repellors evolve symmetrically from limit cycles to chaos when the variable x is replaced with the same function. Totally different bifurcations occur in Figs. 12(c) and 12(d) when the functions of the variable x are slightly unbalanced.

5. Discussion and Conclusions

A dynamical system may display various properties related to their symmetry including coexisting attractors or multiscroll manifold [Zhang & Wang, 2019a, 2019b]. Symmetry or conditional symmetry may exist in forward or backward time. Time-reversible systems provide a new regime of dynamical flows providing time-reversed signals for possible engineering applications [Hoover, 1995]. The coexisting attractors/repellors can merge in the same structure with the same or different phase. Although time-reversible symmetric systems can be obtained from symmetric systems, it is still a new challenge to obtain simple and elegant time-reversible versions with symmetry and conditional symmetry. Our study finds that some simple chaotic systems belong to a special structure with a conditional symmetric repellor if the polarity balance is obtained through offset boosting. In this way, asymmetric attractor and repellor bifurcations are revealed if mismatched offset constants are introduced with different terms.

Acknowledgments

This work was supported financially by the National Nature Science Foundation of China (Grant Nos. 61871230 and 51974045,), the Natural Science Foundation of Jiangsu Province (Grant No. BK20181410), the Startup Foundation for Introducing Talent of NUIST (Grant No. 2016205), and a project funded by the Priority Academic

Program Development of Jiangsu Higher Education Institutions.

References

Bao, B., Li, Q., Wang, N. & Xu, Q. [2016] "Multistability in Chua's circuit with two stable node-foci," *Chaos* **26**, 043111.

Bao, H., Wang, N., Bao, B., Chen, M., Jin, P. & Wang, G. [2018] "Initial condition-dependent dynamics and transient period in memristor-based hypogenetic jerk system with four line equilibria," *Commun. Nonlin. Sci. Numer. Simulat.* **57**, 264–275.

Chen, M., Xu, Q., Lin, Y. & Bao, B. [2017] "Multistability induced by two symmetric stable node-foci in modified canonical Chua's circuit," *Nonlin. Dyn.* **87**, 789–802.

Hoover, W. G. [1995] "Remark on 'some simple chaotic flows'," *Phys. Rev. E* **51**, 759–760.

Hoover, W. G., Kum, O. & Posch, H. A. [1996] "Time-reversible dissipative ergodic maps," *Phys. Rev. E* **53**, 2123–2129.

Jafari, S., Sprott, J. C. & Nazarimehr, F. [2015] "Recent new examples of hidden attractors," *Eur. Phys. J. Spec. Top.* **224**, 1469–1476.

Kuznetsov, N. V., Leonov, G. A., Mokaev, T. N., Prasad, A. & Shrimali, M. D. [2018a] "Finite-time Lyapunov dimension and hidden attractor of the Rabinovich system," *Nonlin. Dyn.* **92**, 267–285.

Kuznetsov, N. V., Leonov, G. A., Mokaev, T. N., Prasad, A. & Shrimali, M. D. [2018b] "Numerical analysis of dynamical systems: Unstable periodic orbits, hidden transient chaotic sets, hidden attractors, and finite-time Lyapunov dimension," *J. Phys.: Conf. Ser.* **1205**, 012034.

Lai, Q. & Chen, S. [2016a] "Generating multiple chaotic attractors from Sprott B system," *Int. J. Bifurcation and Chaos* **26**, 1650177.

Lai, Q. & Chen, S. [2016b] "Research on a new 3D autonomous chaotic system with coexisting attractors," *Optik* **127**, 3000–3004.

Lai, Q., Akif, A., Zhao, X. & Pei, H. [2017] "Various types of coexisting attractors in a new 4D autonomous chaotic system," *Int. J. Bifurcation and Chaos* **27**, 1750142.

Leonov, G. A. & Kuznetsov, N. V. [2015] "On differences and similarities in the analysis of Lorenz, Chen, and Lü systems," *Appl. Math. Comput.* **256**, 334–343.

Leonov, G. A., Kuznetsov, N. V. & Mokaev, T. N. [2015] "Homoclinic orbits, and self-excited and hidden attractors in a Lorenz-like system describing convective fluid motion," *Eur. Phys. J. Spec. Top.* **224**, 1421–1458.

Li, C., Sprott, J. C. & Xing, H. [2016] "Hypogenetic chaotic jerk flows," *Phys. Lett. A* **380**, 1172–1177.

Li, C. & Sprott, J. C. [2016a] "Variable-boostable chaotic flows," *Optik* **127**, 10389–10398.

Li, C. & Sprott, J. C. [2016b] "How to bridge attractors and repellors," *Int. J. Bifurcation and Chaos* **27**, 1750149-1–11.

Li, C., Sprott, J. C. & Xing, H. [2017] "Constructing chaotic systems with conditional symmetry," *Nonlin. Dyn.* **87**, 1351–1358.

Li, C., Sprott, J. C., Liu, Y., Gu, Z. & Zhang, J. [2018] "Offset boosting for breeding conditional symmetry," *Int. J. Bifurcation and Chaos* **28**, 1850163-1–13.

Li, C., Xu, Y., Chen, G., Liu, Y. & Zheng, J. [2019] "Conditional symmetry: Bond for attractor growing," *Nonlin. Dyn.* **95**, 1245–1256.

Liu, Y. & Pang, G. [2011] "The basin of attraction of the Liu system," *Commun. Nonlin. Sci. Numer. Simulat.* **16**, 2065–2071.

Sprott, J. C. [2014] "Simplest chaotic flows with involutional symmetries," *Int. J. Bifurcation and Chaos* **24**, 1450009.

Sprott, J. C. [2015] "Symmetric time-reversible flows with a strange attractor," *Int. J. Bifurcation and Chaos* **25**, 1550078.

Wang, C., Liu, X. & Xia, H. [2017] "Multi-piecewise quadratic nonlinearity memristor and its $2N$-scroll and $2N+1$-scroll chaotic attractors system," *Chaos* **27**, 033114.

Wei, Z., Wang, R. & Liu, A. [2014] "A new finding of the existence of hidden hyperchaotic attractors with no equilibria," *Math. Comput. Simulat.* **100**, 13–23.

Zhang, X. & Wang, C. [2019a] "Multiscroll hyperchaotic system with hidden attractors and its circuit implementation," *Int. J. Bifurcation and Chaos* **29**, 1950117.

Zhang, X. & Wang, C. [2019b] "A novel multi-attractor period multi-scroll chaotic integrated circuit based on CMOS wide adjustable CCCII," *IEEE Access* **7**, 16336–16350.

Zhou, L., Wang, C. & Zhou, L. [2016] "Generating hyperchaotic multi-wing attractor in a 4D memristive circuit," *Nonlin. Dyn.* **85**, 2653–2663.

Zhou, L., Wang, C. & Zhou, L. [2017] "Generating four-wing hyperchaotic attractor and two-wing, three-wing, and four-wing chaotic attractors in 4D memristive system," *Int. J. Bifurcation and Chaos* **27**, 1750027.

Zhou, L., Wang, C., Zhang, X. & Yao, W. [2018a] "Various attractors, coexisting attractors and antimonotonicity in a simple fourth-order memristive twin-T oscillator," *Int. J. Bifurcation and Chaos* **28**, 1850050.

Zhou, L., Wang, C. & Zhou, L. [2018b] "A novel no-equilibrium hyperchaotic multi-wing system via introducing memristor," *Int. J. Circ. Th. Appl.* **46**, 84–98.